Electronic Supplementary Material (ESI) for Physical Chemistry Chemical Physics.

Supplementary Information

How to Characterize Interfacial Load Transfer in Spiral Carbon-Based Nanostructures-Reinforcement Nanocomposites: Is This a Geometry-Dependent Process?

Ali Sharifian,[1] Mostafa Baghani,[1] Gregory M. Odegard,[2] Jianyang Wu,[3,4] Adri C. T. van Duin,[5] and Majid Baniassadi[1,6,*]

[1] School of Mechanical Engineering College of Engineering University of Tehran 1417466191, P.O. Box 11155-4563, Tehran, Iran

[2] Department of Mechanical Engineering-Engineering Mechanics, Michigan Technological University, Houghton, MI 49931, USA

[3] Department of Physics, Jiujiang Research Institute and Research Institute for Biomimetics and Soft Matter, Fujian Provincial Key Laboratory for Soft Functional Materials Research, Xiamen University, Xiamen 361005, P. R. China

[4] NTNU Nanomechanical Lab, Department of Structural Engineering, Norwegian University of Science and Technology (NTNU), Trondheim 7491, Norway

[5] Department of Mechanical Engineering, Pennsylvania State University, University Park, State College, Pennsylvania 16801, USA

[6] University of Strasbourg ICube/CNRS, 2 Rue Boussingault, 6700 Strasbourg France

---

[*] Corresponding author at: Mech, Eng. Dept. College of Engineering, University of Tehran, Iran. Tel: +98 21 88024035; fax: +98 21 8801 3029.
Email: m.baniassadi@ut.ac.ir

Table of Contents

S1. Utilization of graphene as a representative interface element. 4

S2. The pull-out test of graphene. 5

S3. Performing the pull-out test of (2,1,2,1) CCNT fully embedded in polyethylene matrix. 7

S4. Investigation of the SCBN pull-out velocity effects on separation behavior. 9

S5. Investigation of the averaging time interval effects on separation behavior. 10

S6. The pull-out test in normal mode separation for (2,1,2,1) CCNT. 11

S7. Further details for the sliding mode separation of the (2,1,2,1) CCNT. 12

S8. Sliding mode separation behavior of (2,1,2,1) SCBN embedded in polyethylene chains of C110H222. 13

S9. Atomistic configurations of (2,0,4,0) and (3,1,7,1) SCBNs, and polyethylene chains within structures. 14

S10. Further details for the sliding mode separation of the (6,1,2,1) CCNT. 15

S11. The pull-out test in sliding mode separation for (2,1,2,1) SCBN with 3, 4 and 6 coils. 16

S12. Compression of the polyethylene box surrounding the (2,1,2,1) SCBN. 18

S13. Functionalization of (2,1,2,1) SCBN by a single polyethylene chain. 19

S14. Comparison of the mechanical properties between the pristine (2,1,2,1) SCBN and the functionalized (2,1,2,1) SCBN by a single polyethylene chain. 20

S15. The analysis of the pull-out test of functionalized (6,1,2,1) SCBN by a single polyethylene chain according to the second method described in “Parameters affecting the separation behavior” section of paper. 21

S16. The analysis of the pull-out test of functionalized (2,1,2,1) SCBN by a single polyethylene chain according to the second method described in the “Parameters affecting the separation behavior” of paper. 23

S17. Investigation of the stress per atom of (3,1,7,1) SCBN and (2,1,2,1) SCBN during the pull-out test process. 25

S18. Determine the selected area during pull-out test in normal and sliding modes. 26

S19. The pull-out test of CNT with chirality of (8,0) in sliding mode separation. 28

S20. The unconstrained/constrained area of simulation box during pullout test. 30

References 32

S1. Utilization of graphene as a representative interface element.

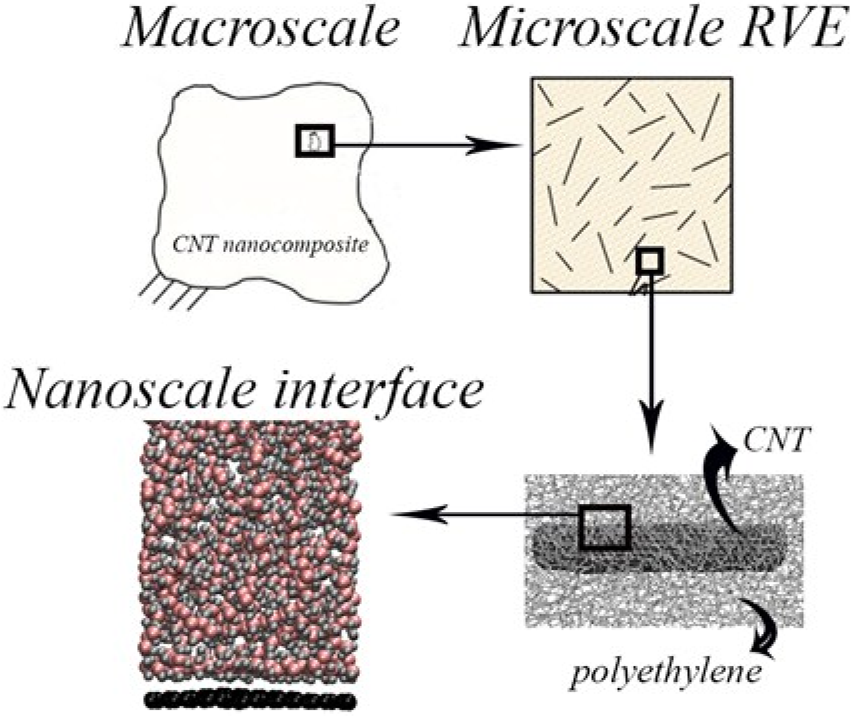

Figure S 1. Mechanical behavior of CNT/graphene reinforcement nanocomposites with interfacial effect which is result of graphene as a representative nanoscale interface element.

S2. The pull-out test of graphene.

The graphene with size of 24 × 25 A^2 is embedded in CH3-(CH2)78-CH3 (for discussion convince is denoted as C80H162) polyethylene chains with 70% of the unconstrained matrix box region as indicated in Figure S 2. The size of the polyethylene box is 25 × 24 × 46 A^3. For simplicity, the polyethylene chains are placed in a simulation box of the appropriate density[1-4] of 1.1 $^{g}/_{cm^3}$ by packing module[5] of Materials Studio software package. The system reaches the equilibrium state under the NVT and NPT ensembles, respectively, based on Nosé–Hoover thermostat and Nosé–Hoover barostat at a temperature of 100 K and a pressure of 1 atm. Also, after applying the constrained region, the NVT ensemble based on Nosé–Hoover thermostat is used at a temperature of 100 K (which is far from the glass temperature (250 K) of polyethylene[6]) for equilibration. Then the pull-out test is performed at an appropriate[1, 2, 4, 7] constant velocity of 0.000025 A/fs. The AIREBO potential[8] has been used to simulate long-range and short-range interactions of carbon and hydrogen atoms, as in previous researches[1, 9-12]. During the pull-out simulation, the NVT ensemble based on Nosé–Hoover thermostat is used at a temperature of 100 K. The periodic boundary condition is applied in all directions except the normal separation direction. The force per carbon atoms for the graphene is averaged over every 4 ps and is reported along with the displacement in Figure S 2. In order to maintain the original shape of the nanostructure, the whole nanostructure has been fixed. It is concluded that the normal mode separation of graphene involves three stages. In the first stage, the force per atom increases dramatically to about 2 Angstroms. Following the process of separation and accompanied by formation of cavities in polyethylene, the force gradually decreases in the second stage. In the third stage, the force is almost zero, and the interaction between polyethylene chain and graphene has almost disappeared. The maximum force, separation energy and separation distance for the sample are calculated to be 5.8 pN, 204.6 mJ/m^2 and 47 A, respectively, which are in agreement with the previous researches[1-3]. The graphene pull-out test results have been used in many macroscale simulations for calculating effective properties of carbon-based material/polyethylene nanocomposites [14 ,13 ,2 ,1].

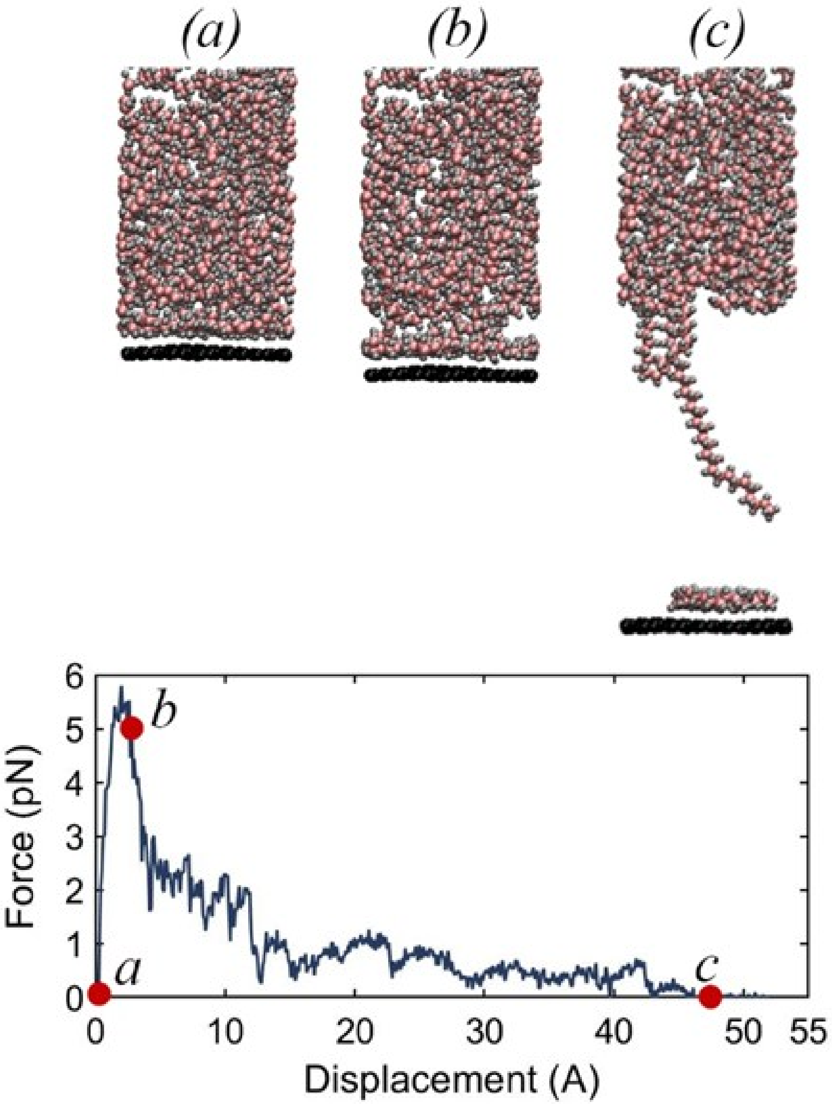

Figure S 2. The force per atom-displacement diagram for normal mode separation of graphene. The interaction of graphene and polyethylene is shown in different displacements.

S3. Performing the pull-out test of (2,1,2,1) CCNT fully embedded in polyethylene matrix.

The pull-out test in sliding mode separation is performed for (2,1,2,1) CCNT fully embedded in polyethylene matrix. This is due to consideration of the normal separation effect of special area of SCBN as shown in Figure S 3b. All conditions are the same as in the **“sliding mode separation”** section of paper. As the results show, the maximum force for separation has increased in the first and second stages. This is the result of the normal separation effect, which is relatively small (about 1 pN) due to the low thickness of the CCNT. Also, the free boundary condition is applied on both sides of the pull-out test direction, while, applying the constrained area condition in the region shown in Figure S 3a, will lead to the increase in force. Also, as demonstrated in Figure S 3d, the opening of the coils with respect to each other does not occur at fully embedded CCNT. However, this can be predicted, for example, by comparing the separation force and the force required to open the coils in the absence of polyethylene (mechanical properties of the SCBNs[15, 16]). Based on the results, it can be stated that the boundary condition applied in **“sliding mode separation”** section of paper provides reasonable results.

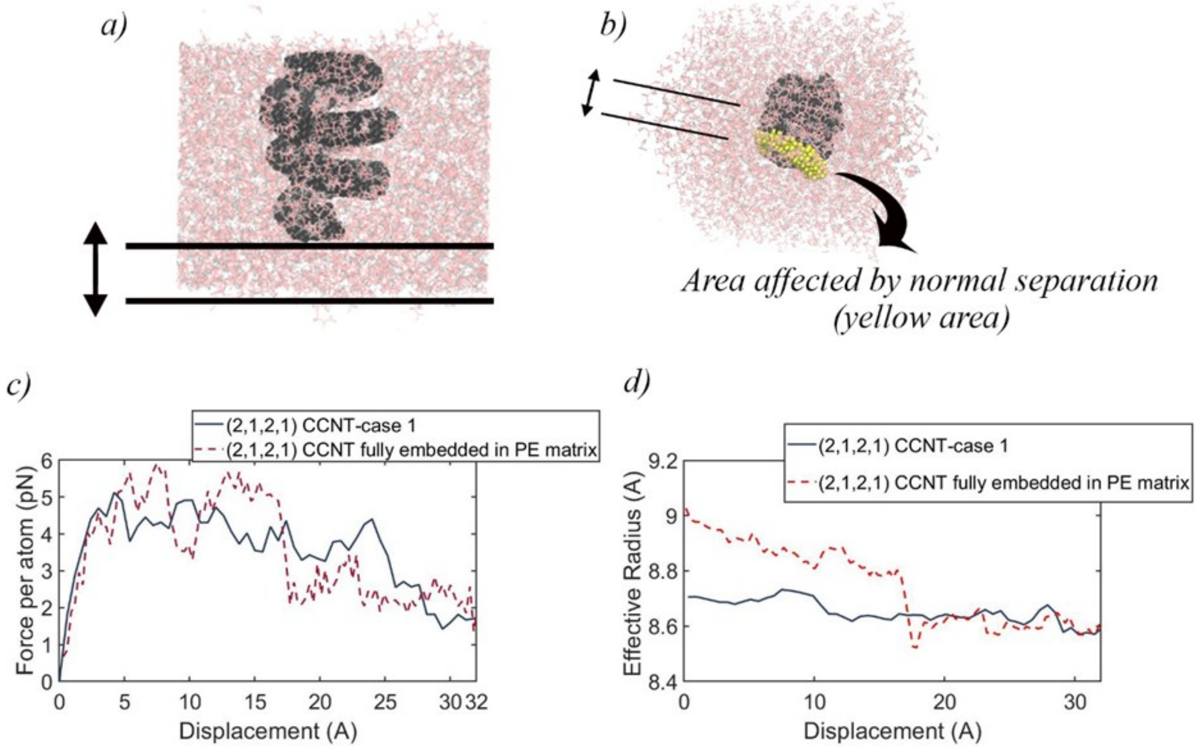

Figure S 3. Investigating the pull-out test of (2,1,2,1) CCNT fully embedded in polyethylene matrix. (a,b) atomistic configuration of ((2,1,2,1) CCNT fully embedded in polyethylene matrix. Comparing separation behavior of (2,1,2,1) CCNT fully embedded in polyethylene and (2,1,2,1) CCNT case1 of ***"sliding mode separation"*** *of paper by (c) force per atom-displacement diagram, and (d) effective radius-displacement diagram.*

S4. Investigation of the SCBN[1] pull-out velocity effects on separation behavior.

This section examines the pull-out velocity of the SCBNs in sliding mode separation. For this purpose, the velocities of 0.000025 A/fs, 0.00015 A/fs, and 0.00025 A/fs have been selected. The velocities of 0.000025 A/fs and 0.00015 A/fs are known as appropriate velocity in previous studies for graphene pull-out test (which has fewer atoms and a smaller surface compared to SCBNs). The pull-out test is performed for all three velocities according to the method described in **"sliding mode separation"** section of paper for (2,1,2,1) CCNT with three coils (full specifications in Table 1 of the paper). The force per carbon atom for the studied region of the SCBN is averaged over every 4 ps. Consequently, for lower velocities, smaller displacements account for a mean value of the force that can lead to more fluctuations as shown in Figure S 4. As depicted in Figure S 4, a similar separation behavior can be observed in all three pull-out velocities, and this amount of difference, according to previous researches, is also logical[7 ,3-1]. Maximum force, displacement and separation energy are respectively obtained by increasing the mentioned velocities: 5.4150 pN, 5.5651 pN, 6.0126 pN, 60 A, 60 A, 61 A, 479.5946 mJ/m^2,514.8461 mJ/

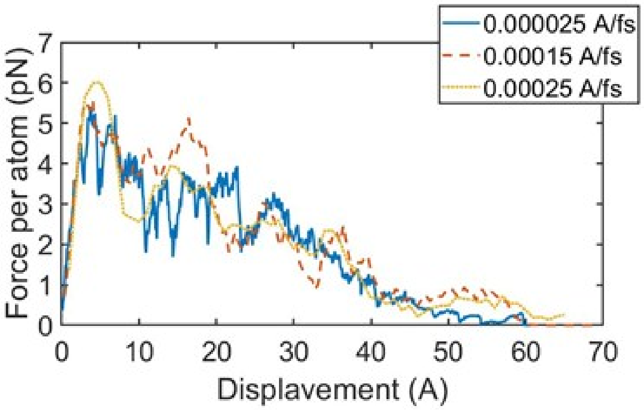

Figure S 4. Force per atom-displacement diagram for the velocities of 0.000025 A/fs, 0.00015 A/fs, and 0.00025 A/fs.

---

[1] Spiral Carbon-Based Nanostructure

m^2, 463.3326 mJ/m^2. The similarity of the results indicates the reliability of all three velocities for the pull-out test, although the 0.00015 A/fs is applied in the pull-out test.

S5. Investigation of the averaging time interval effects on separation behavior.

In order to examine the relationship between the averaging time interval and the separation behavior of graphene, the pull-out test is performed similarly to the method described in the section "**S2-The pull-out test of graphene from polyethylene matrix"** of manuscript in the averaging intervals of every 2 ps and 4 ps. As shown in the Figure S 5, both graphs display the same behavior. The maximum force and separation energy with increasing averaging time intervals are 5.3574 pN, 5.8011 pN, 203.4527 mJ/$m^2$and 195.1927 mJ/m^2, respectively.

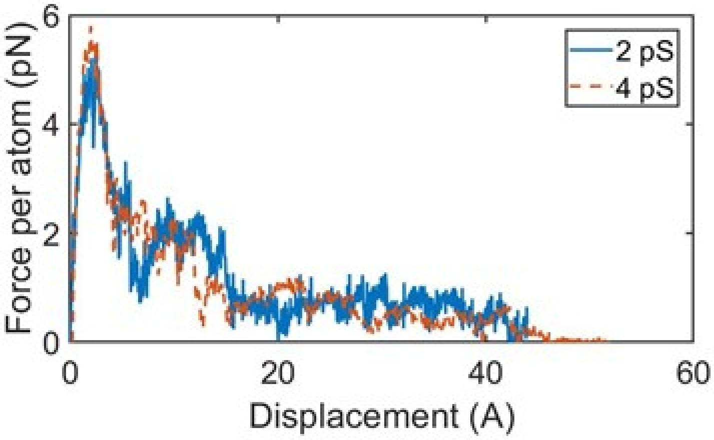

Figure S 5.Force per atom-displacement diagram for the averaging time intervals of 2ps and 4ps.

S6. The pull-out test in normal mode separation for (2,1,2,1) CCNT.

As discussed in the **“normal mode separation”** section of the paper, if the entire upper region of the SCBNs (for discussion convince is denoted as sample B) is selected as the study area, the sliding mode separation will occur in the corner of the structure as shown in Figure 2. Consequently, this reduces the severity of the normal mode separation force. As shown in the Figure S 6, with the selection of the entire upper segment of SCBN as studied area, the overall separation behavior of nanoparticle has not changed, and the observed stages are the same as the cases examined in the **“normal mode separation”** section of paper (for discussion convince is denoted as sample A). The maximum forces for both samples are approximately equal, but there is a significant difference in separation energy. So that in higher displacements, there is a reduction in force for sample B. The separation energy for the sample B is 653.7841 mJ/m^2, which is 39% lower than the previous one. According to Figure 2, the reason for the tangible reduction of energy is that the separation after the first stage is extremely rapid in the corners of the structure, and the corners are rapidly separated from the polyethylene (due to the sliding mode separation). Since this section provides general information about the normal separation analysis, then the results can be utilized to suit any other model. Although the examined model in the **“normal mode separation”** of the paper seems to be more precise.

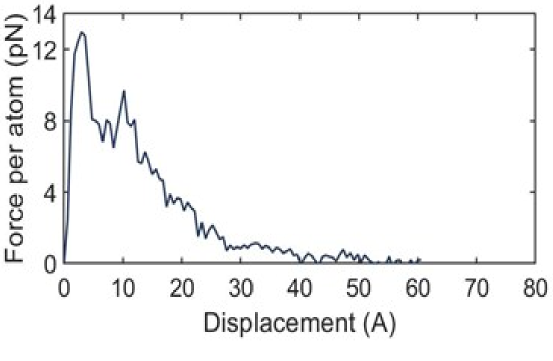

Figure S 6. The force per atom-displacement diagram for normal mode separation of sample B.

S7. Further details for the sliding mode separation of the (2,1,2,1) CCNT.

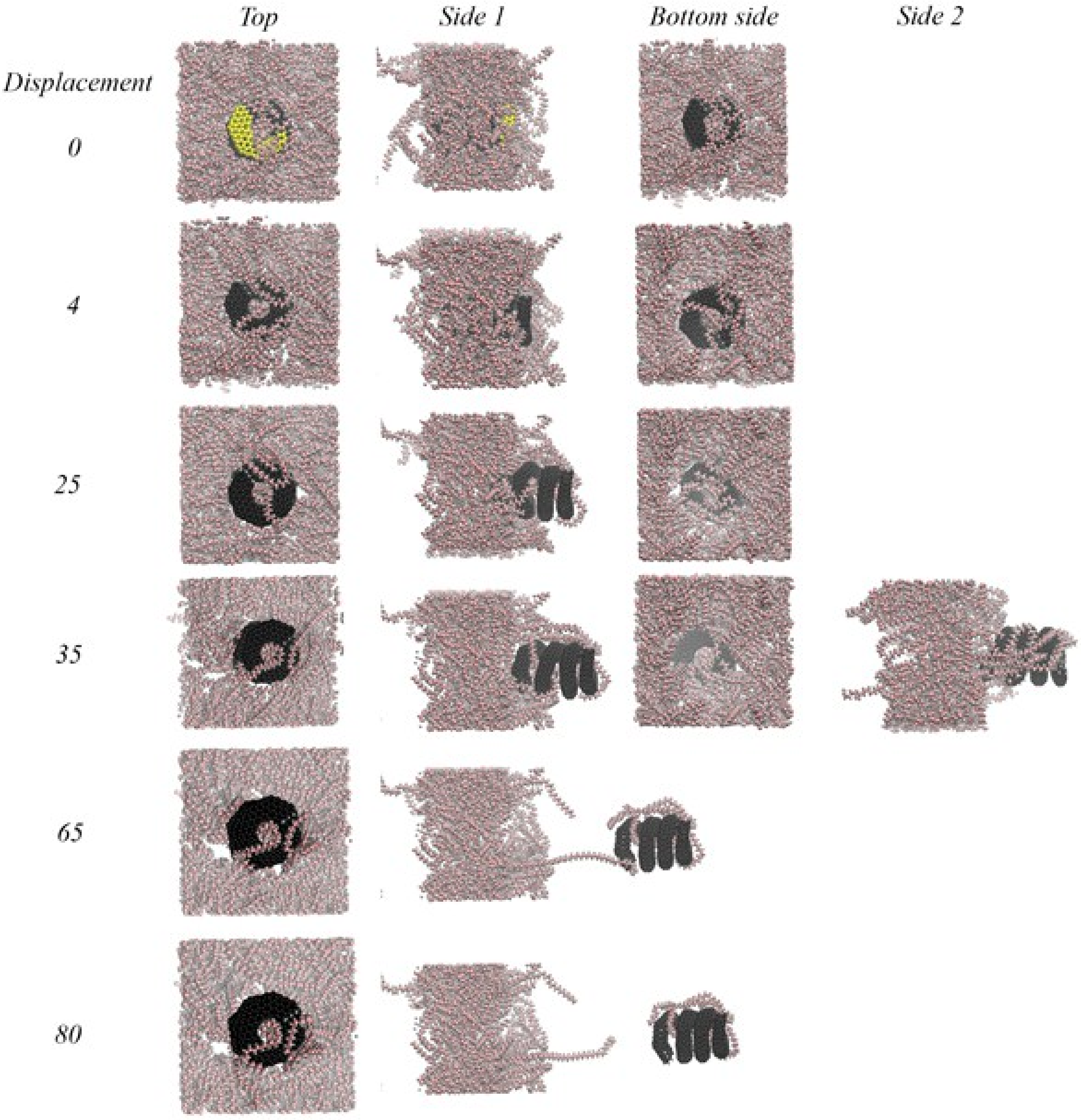

Figure S 7. Atomistic configuration of (2,1,2,1) SCBN in sliding mode separation.

S8. Sliding mode separation behavior of (2,1,2,1) SCBN embedded in polyethylene chains of C110H222.

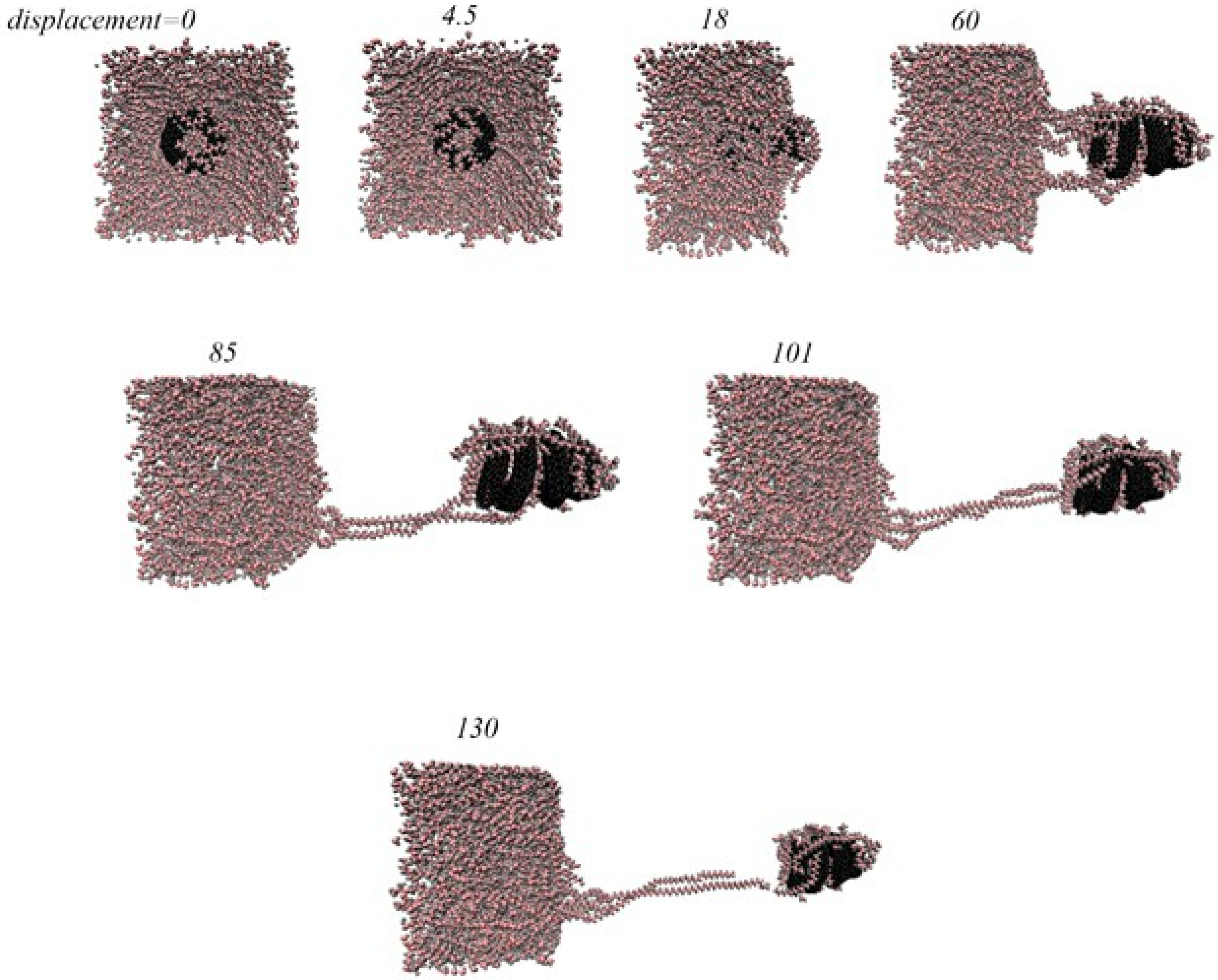

Figure S 8. Sliding mode separation behavior of (2,1,2,1) SCBN embedded in polyethylene chains of C110H222.

S9. Atomistic configurations of (2,0,4,0) and (3,1,7,1) SCBNs, and polyethylene chains within structures.

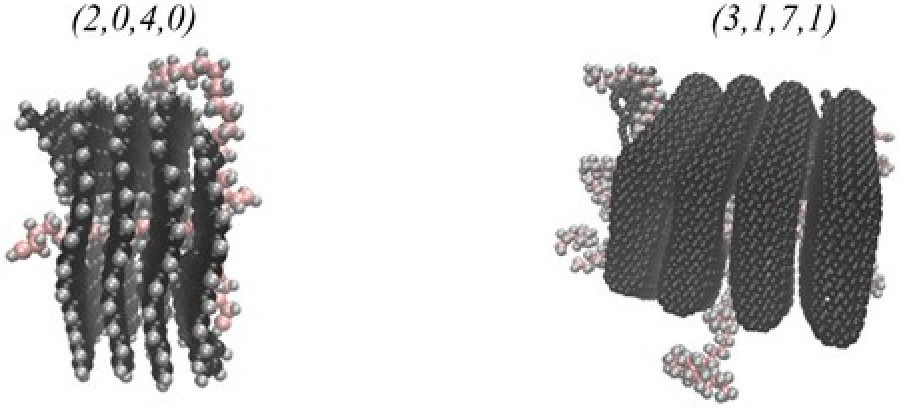

Figure S 9. The display of (2,0,4,0) and (3,1,7,1) SCBNs, and polyethylene chains within structures.

S10. Further details for the sliding mode separation of the (6,1,2,1) CCNT.

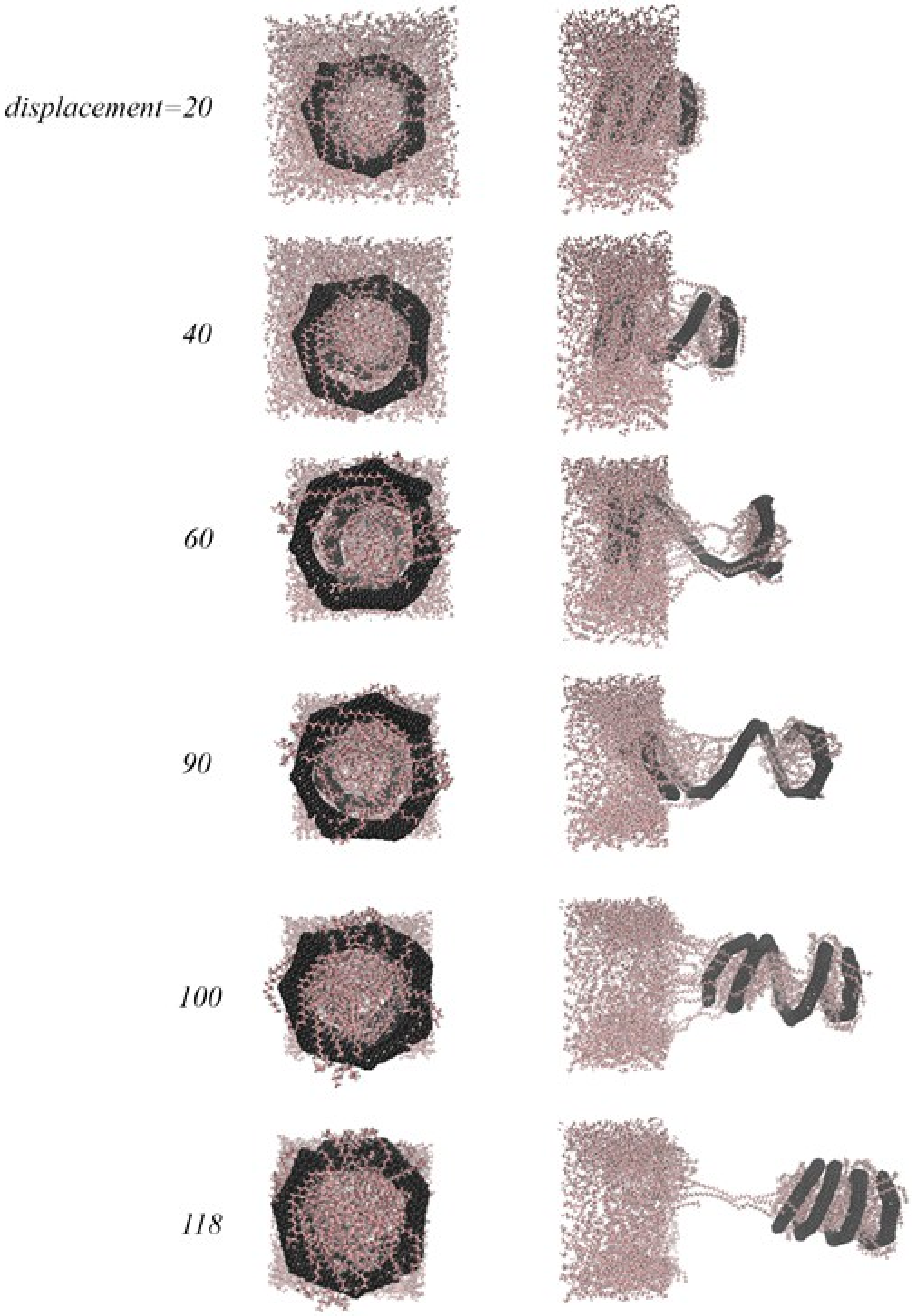

Figure S 10. Atomistic configuration of (6,1,2,1) SCBN in sliding mode separation.

S11. The pull-out test in sliding mode separation for (2,1,2,1) SCBN with 3, 4 and 6 coils.

By observing the Figure S 11, The complete similarity of the separation behavior stages for (2,1,2,1) SCBN with 3, 4, and 6 coils is demonstrated in Figure S 11. This declares that the size of the studied nanoparticles is large enough to produce the same results. Although a small difference in the results can be due to the initial configurations, as expressed in the **"sliding mode separation"** of the paper. Also, for the precise comparison of separation energy, the length of nanostructures embedded in the polyethylene chains in the direction of pull-out should be calculated as a parameter. Because the effect of width is eliminated by dividing the energy of the separation onto the surface, although the separation energy increases with raising the length of nanostructures embedded in the polyethylene chains. Thus, by dividing energy per area over the length of nanostructure, a comparable quantity is obtained. In some studies, the results have been compared with the calculation of the interfacial shear strength (ISS), which one may culminate to be non-dimensional related to the length of the nanostructure. Due to the geometric complexity of spiral structures and also obtaining more precise results, this method has not been used. Therefore, the Table S 1 shows the maximum force, separation energy and separation energy per initial length of the nanostructure which obtains a better insight into the comparison of the results. With respect to Figure S 11, it can be seen that for a SCBN with six coils in the stage 1, firstly, the force goes far beyond the other two samples, and then reaches a value equal to the two. The reason of this can be deduced from the number of coils. Because of the transfer of power from the first coils to the last coils. Due to the flexibility of the coils and the length of the SCBN, a slight oscillation is observed. Then, the rest of the path is similar to the two ones.

Table S 1. Force per atom, separation energy and final displacement for (2,1,2,1) CCNT with 3,4 and 6 coils.

Structural type (s,n77,n75,n55)	**condition**	**Max-Force per atom (pN)**	**Initial length (A)**	**Separation Energy (mJ/m^2)**	**Max-Traction (GPa)**	**Final displacement (A)**	**Separation Energy per initial length (mJ/m^3)**
(2,1,2,1)	4 coils	5.1264	31	526.8848	0.19571	80	16.996284
(2,1,2,1)	3 coils	5.5651	28	514.8461	0.21	60	18.387361
(2,1,2,1)	6 coils	8.6528	54	948.3255	0.33	114	17.561583

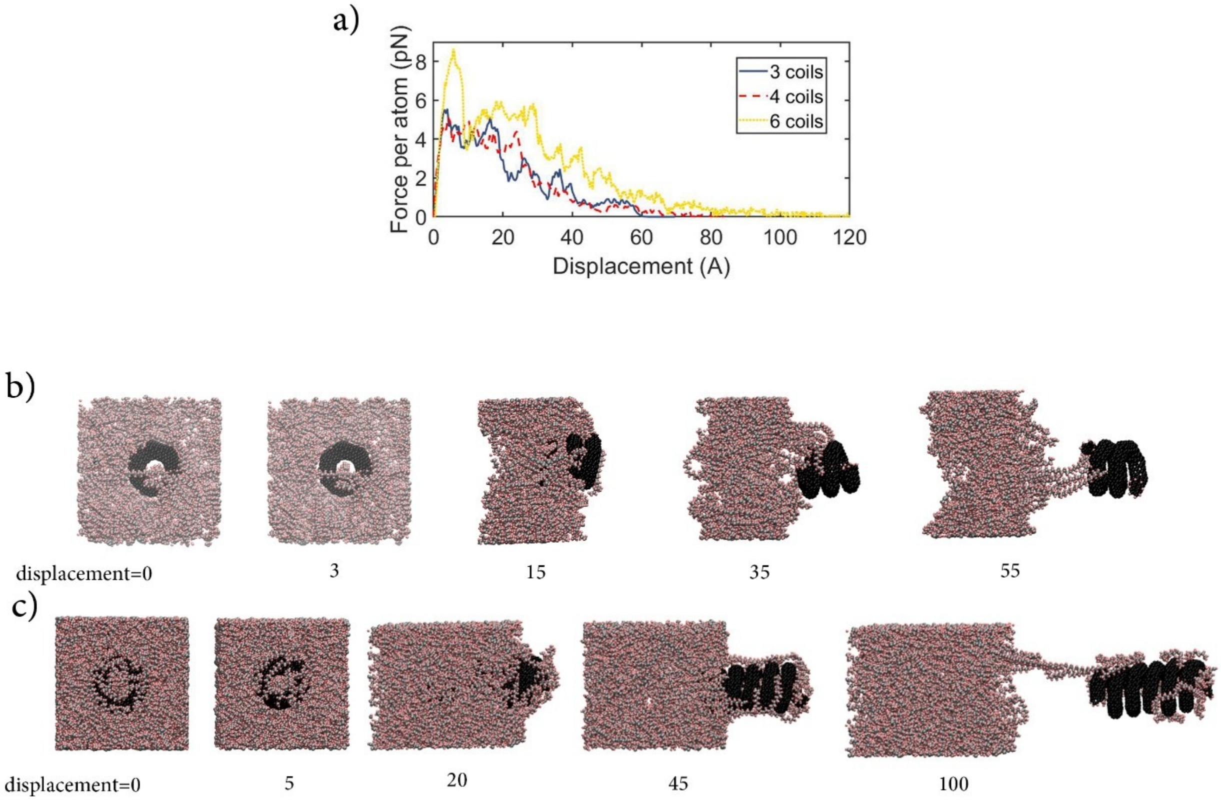

Figure S 11. Sliding mode separation of (2,1,2,1) SCBN with 3, 4 and 6 coils. (a) force per atom-displacement diagram for (2,1,2,1) SCBN with 3, 4 and 6 coils. Atomistic configurations for (2,1,2,1) SCBN with, (b) 3 coils, and, (c) 6 coils.

S12. Compression of the polyethylene box surrounding the (2,1,2,1) SCBN.

As shown in Figure S 12, the fixed region of the polyethylene chain box is moved towards the center. This process takes place in both directions perpendicular to the pull-out direction.

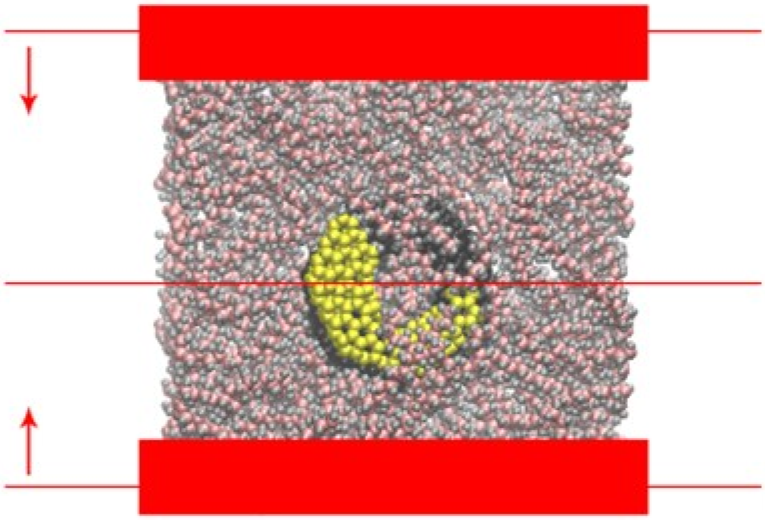

Figure S 12. Compression of the polyethylene box surrounding the (2, 1, 2, 1) SCBN.

S13. Functionalization of (2,1,2,1) SCBN by a single polyethylene chain.

The structure of functionalized SCBN by a polyethylene chain of C80H162 is exhibited in two different views.

S14. Comparison of the mechanical properties between the pristine (2,1,2,1) SCBN and the functionalized (2,1,2,1) SCBN by a single polyethylene chain.

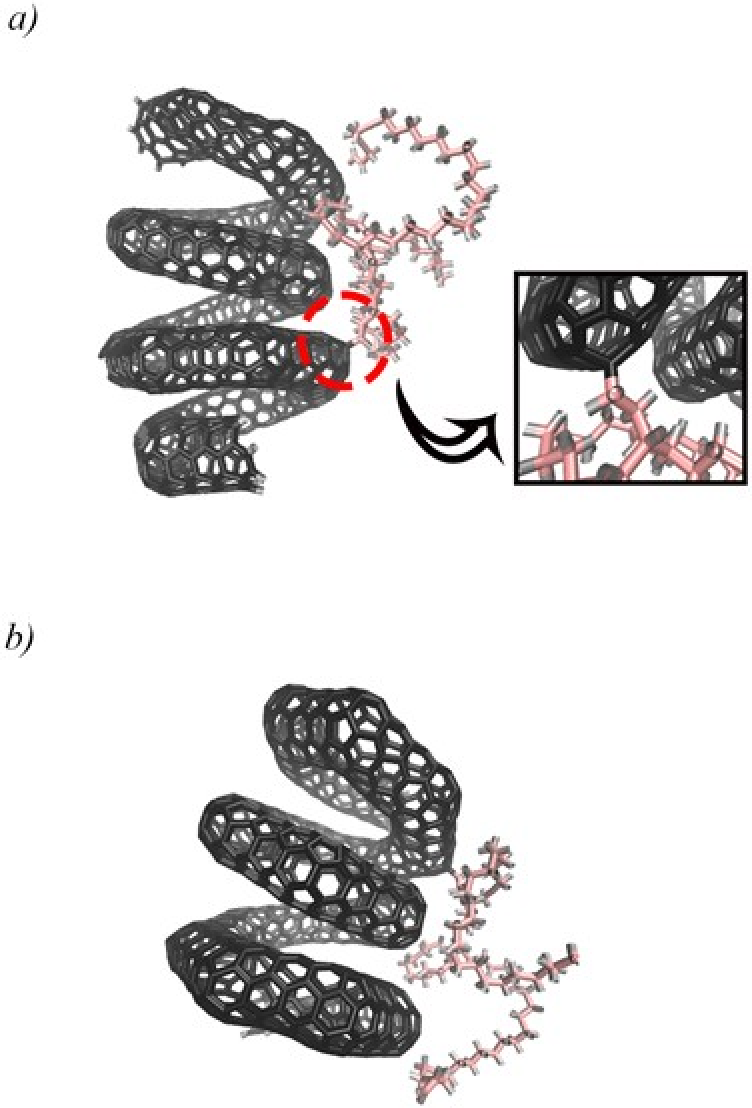

Figure S 13. Functionalized (2,1,2,1) SCBN by a polyethylene chain of C80H162 is shown in two different views.

In order to investigate the effect of functionalization of (2,1,2,1) SCBN by a polyethylene chain on mechanical properties, the tensile test for both pristine and functionalized structures is performed according to the conditions stated in previous studies[17 ,15]. The examined strain interval is between 0 and 1, which is actually much larger than the strain observed in the pull-out process. As shown in Figure S 14, the trend of two graphs are quite similar to each other. Also, snapshots of the behavior of both structures are shown in Figure S 14. Atomic configurations of functionalized SCBN are characterized as bold and atomic configurations of pristine SCBN are presented colorless in various strains. The similarity of the mechanical response of both structures indicates that the functionalization is not affected by a single polyethylene chain.

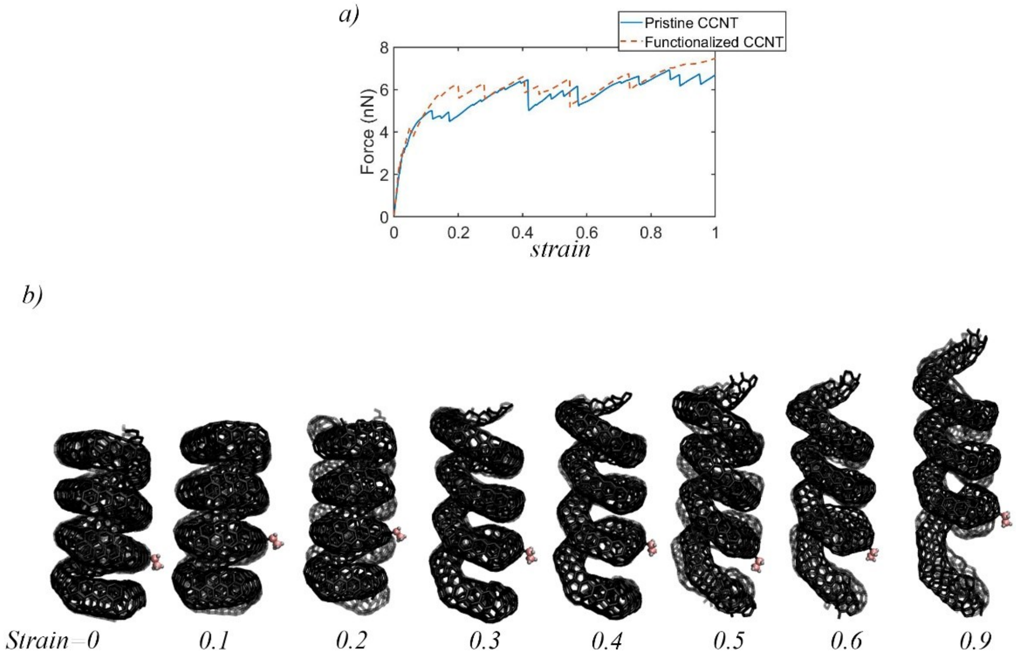

Figure S 14. Comparison of the mechanical properties of the pristine (2,1,2,1) SCBN and the functionalized (2,1,2,1) SCBN by a polyethylene chain. (a) Force-strain diagram for pristine and functionalized SCBNs. (b) Atomistic configuration of pristine (colorless) and functionalized (bold) SCBN in various strains.

S15. The analysis of the pull-out test of functionalized (6,1,2,1) SCBN by a single polyethylene chain according to the second method described in “Parameters affecting the separation behavior” section of paper.

Using the second method described in the **“Parameters affecting the separation behavior”** section of paper, the separation behavior of the functionalized (6.1.2.1) SCBN has been investigated. In the second method, due to the connection of the polyethylene chain to the fixed region of the polyethylene box and nanostructure, nanostructure coils are opened from each other during the separation process. Therefore, a nanoparticle is selected that the effect of the opening of the coils is observed for the pull-out test of the pristine nanoparticle during the separation process. As observed in Figure S 15 and S16, the same separation behavior can be seen up to the displacement of 95 A for pristine and functionalized SCBN. However, when the last coil of SCBN is expelled from polyethylene box, a different behavior is observed due to the connection of the polyethylene chain to the nanostructure and the fixed region of the polyethylene box. As for the pristine nanoparticle, the coils are slowly pulled out, but, for the functionalized nanoparticle, the coils open from each other. Because the force required to tear the polyethylene chain is much more than opening the rings. For this reason, the coils open up to a point where the nanostructure is almost completely straight. The process has continued only to 217 A displacement. Due to the length of the process, it is discontinued. In order to achieve better physical insight, the atomic configurations of nanoparticles and polyethylene chains are shown in Figure S 16.

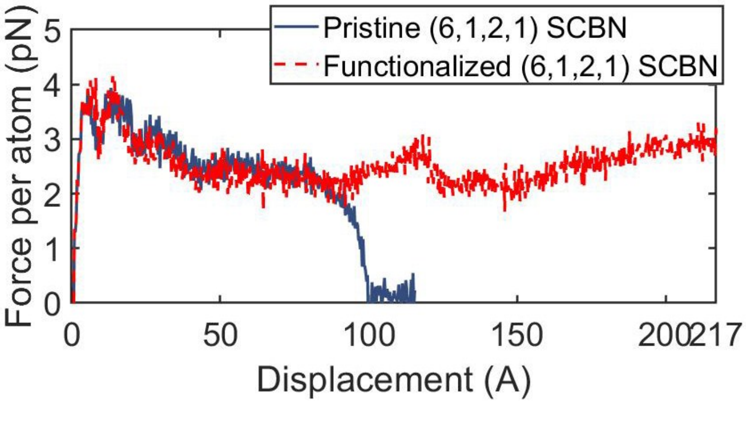

Figure S 15. Force per atom-displacement diagram for pristine and functionalized (6,1,2,1) SCBN.

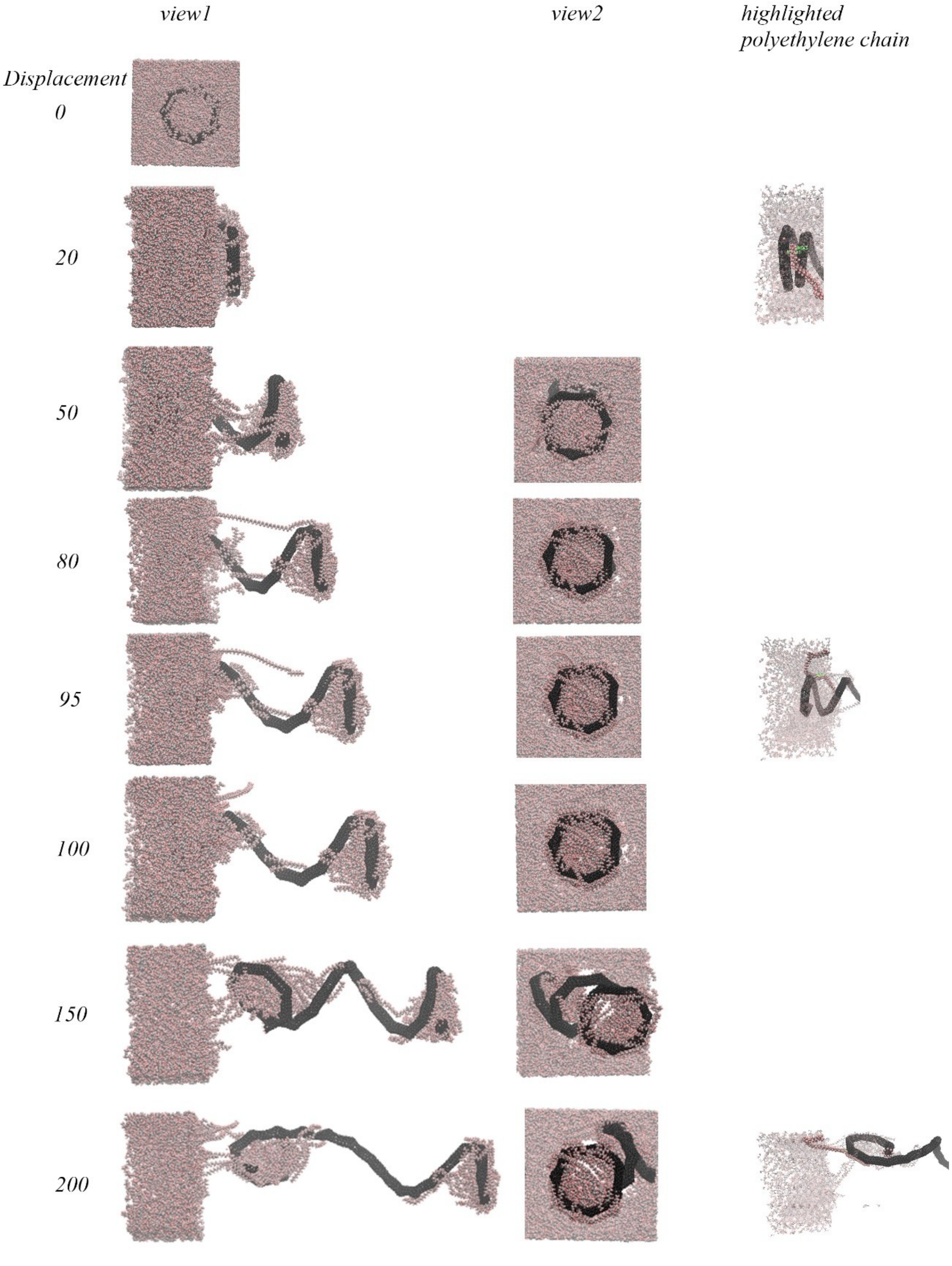

Figure S 16. Atomistic configuration of the pull-out test of functionalized (6,1,2,1) SCBN.

S16. The analysis of the pull-out test of functionalized (2,1,2,1) SCBN by a single polyethylene chain according to the second method described in the “Parameters affecting the separation behavior” of paper.

The pull-out test of (2.1.2.1) SCBN is performed according to the second method described in the **“Parameters affecting the separation behavior”** of paper. As shown in Figure S 17, a similar behavior for pristine and functionalized SCBN is observed up to the displacement of 40 A (the first, second and mid-third stages). After this displacement and stretching a polyethylene chain connected to the functionalized nanoparticle, behavioral differences begin. The coils then slightly open up to a displacement of about 75 A in the final area of SCBN (where the polyethylene chain is attached). In more displacements, the coils open in the entire structure, and eventually the polyethylene chain is torn.

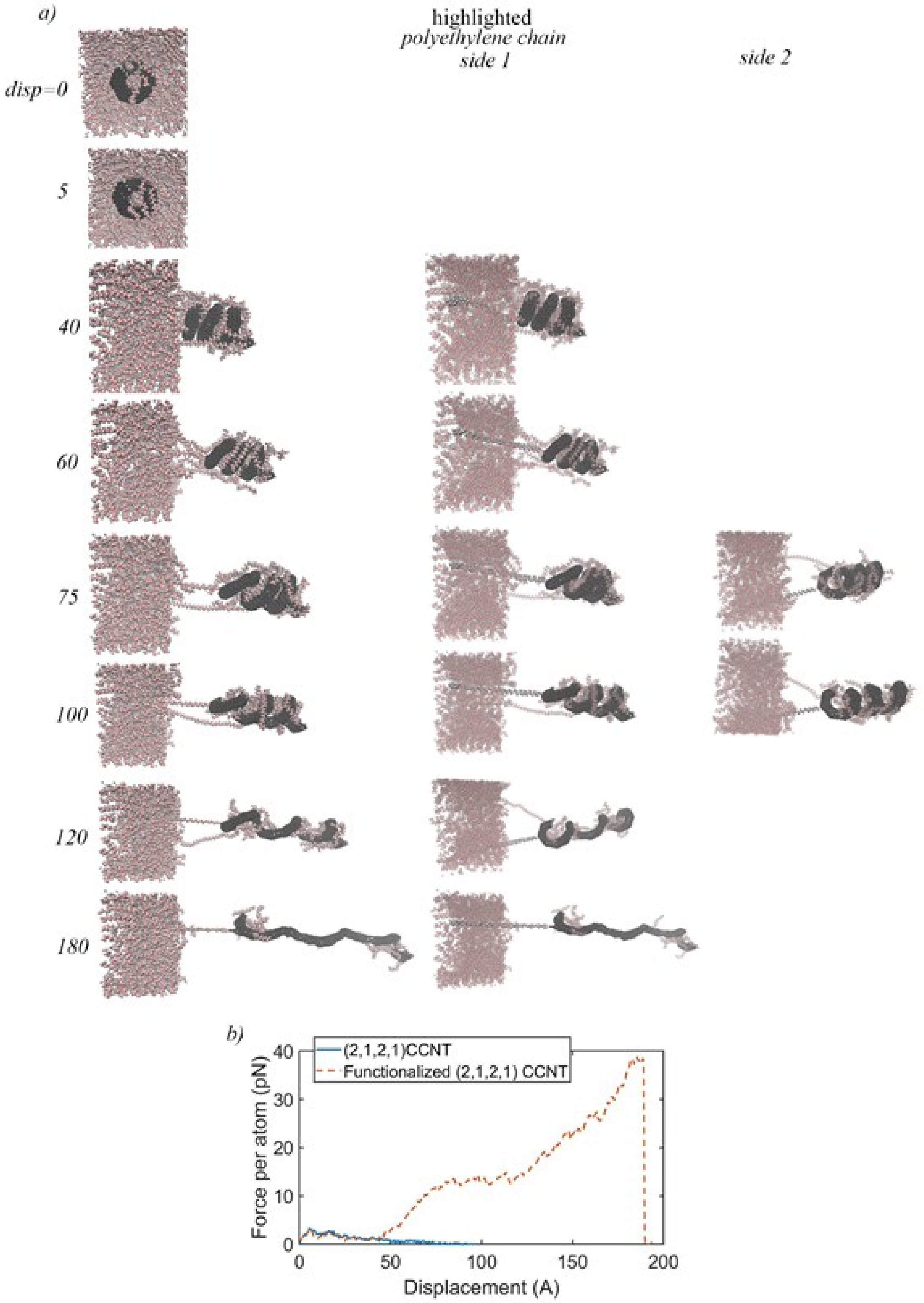

Figure S 17. The pull-out test of functionalized (2,1,2,1) SCBN. (a) Atomistic configuration of the pull-out test of functionalized (2,1,2,1) SCBN. (b) Force per atom-displacement diagram for pristine and functionalized (2,1,2,1) SCBN.

S17. Investigation of the stress per atom of (3,1,7,1) SCBN and (2,1,2,1) SCBN during the pull-out test process.

As indicated Figure S 18, during the pull-out process the stress of nanoparticle in the inner and outer region of the SCBNs is much larger than the other regions. As semi-major increases, this difference is apparent in (3,1,7,1) SCBN. This phenomenon is entirely compatible with the manner in which the studied areas is selected in the pull-out test. Also, the stress of both structures are shown in the second stage of the pull-out test.

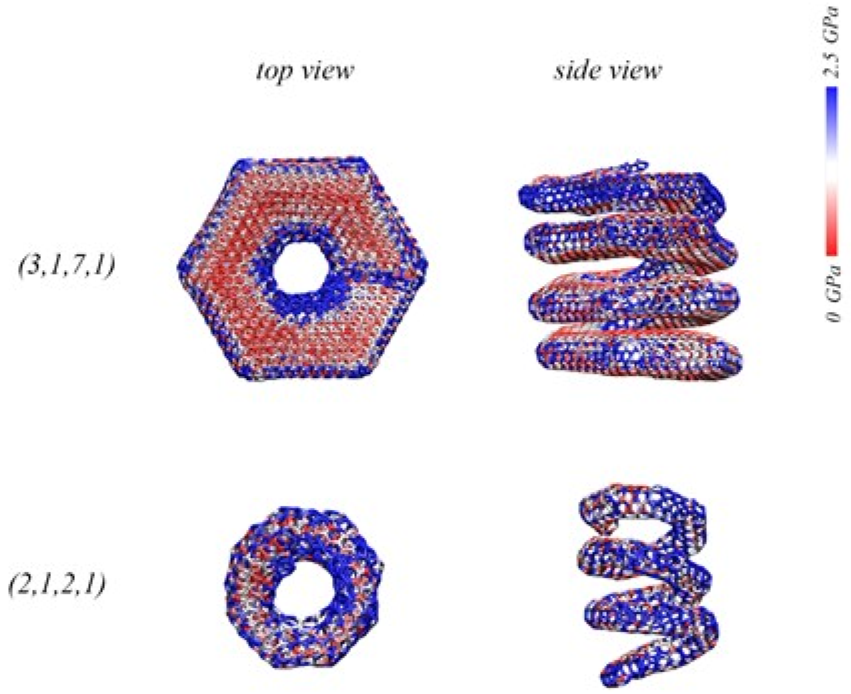

Figure S 18. Investigation of the stress per atom of (3,1,7,1) SCBN and (2,1,2,1) SCBN during the pull-out test process in the second stage of pull-out test.

S18. Determine the selected area during pull-out test in normal and sliding modes.

As shown in Figure S 19b, to eliminate the sliding mode separation effects as well as the effects of the breaking chemical bond of polyethylene chains, a portion of the upper area of the SCBNs is selected for analysis. It is worthnorthy, separation occurs only in the upper part of the selected area. While for spiral structures, the effects of intra-structures polyethylene chains are also so important. As a matter of fact, this is the main difference between these structures and flat structures such as graphene, which has a significant effect on the normal separation behavior. Therefore, the separation forces are calculated for the entire selected area. But the entire force is applied only to the upper part of the selected area for the analysis of the results. (As shown in Figure S 19b)

The area of spiral structures associated with polyethylene chains is selected as the area under study in the sliding mode separation. As shown in Figure S 19c, these areas are inside and outside the structure where separation occurs. Also, the observed stress in these areas (as described in the **“S17. Investigation of the stress per atom of (3,1,7,1) SCBN and (2,1,2,1) SCBN during the pull-out test process.”**) confirm this choice. The marked area with a different color represents the fixed area for the purpose of applying the pull-out test.

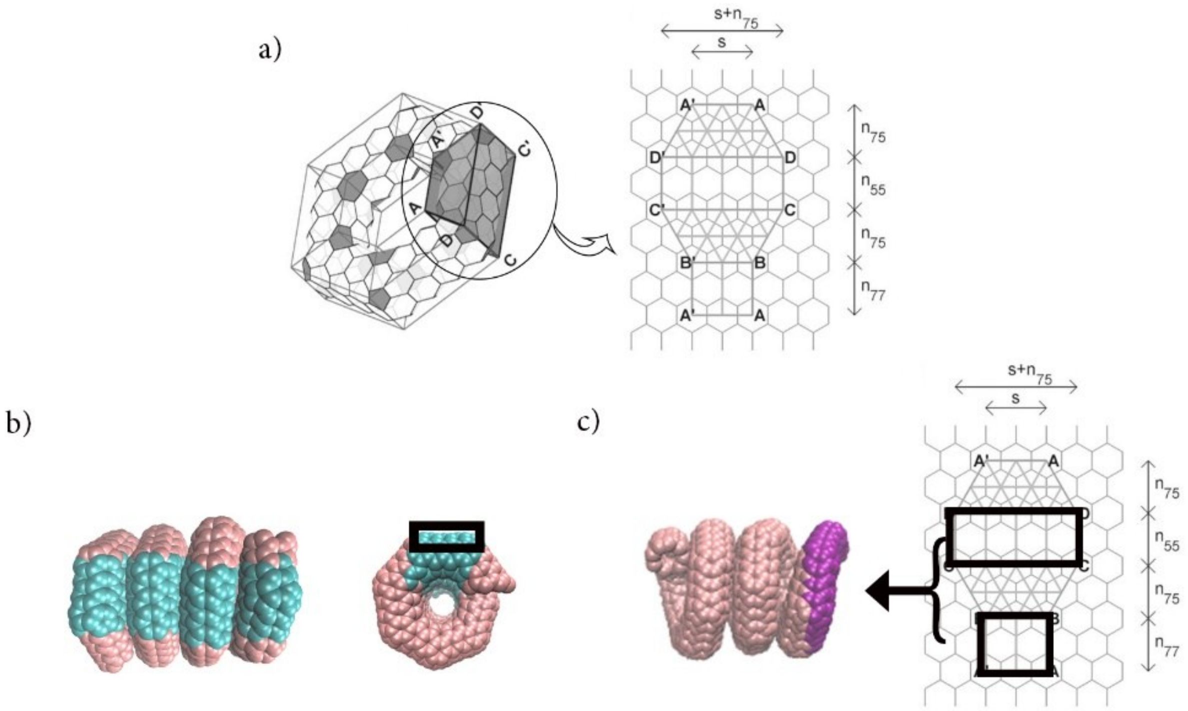

Figure S 19. The selected area during pull-out test in normal and sliding modes. (a) The toroidal carbon nanotube (TCNT) which the produce structure of the corresponded SCBN. The selected area of SCBN in (b) normal mode and (c) sliding mode separation.

Table S 2. Structural characteristics of the SCBNs with four coils.

Structural type (s,n77,n75,n55)	Semi-major (Å)	Semi-minor (Å)	Effective radius (Å)	Inner diameter (Å)	Outer diameter (Å)	Initial length (A)	The number of atoms under study
(2,1,2,1)	2.9	2.65	8.60074	11.5	21.1	31	576
(2,0,4,0)	3.185	0	9.69597	11.41	25.58	22	384
(3,1,7,1)	5.8	3	15.9616	16.2	38.45	52	1248
(6,1,2,1)	2.63	2.7	20.0464	33.1	42.7	37	1344

S19. The pull-out test of CNT with chirality of (8,0) in sliding mode separation.

The CNT with chirality of (8,0) and length of 38A is embedded in C80H162 polyethylene chains with 70% of the unconstrained matrix box region as indicated in Figure S 20. The size of the polyethylene box is 55 × 55 × 38 A^3. For simplicity, the polyethylene chains are placed in a simulation box of the appropriate density[1-4] of 1.1 $^{g}/_{cm^3}$ by packing module[5] of Materials Studio software package. The system reaches the equilibrium state under the NVT and NPT ensembles, respectively, based on Nosé–Hoover thermostat and Nosé–Hoover barostat at a temperature of 100 K and a pressure of 1 atm. Also, after applying the constrained region, the NVT ensemble based on Nosé–Hoover thermostat is used at a temperature of 100 K (which is far from the glass temperature (250 K) of polyethylene[6]) for equilibration. Then the pull-out test is performed at an appropriate[1, 2, 4, 7] constant velocity of 0.00005 A/fs. The AIREBO potential[8] has been used to simulate long-range and short-range interactions of carbon and hydrogen atoms, as in previous researches[1, 9-12]. During the pull-out simulation, the NVT ensemble based on Nosé–Hoover thermostat is used at a temperature of 100 K. The periodic boundary condition is applied in all directions except the normal separation direction. The force per carbon atoms for the graphene is averaged over every 4 ps and is reported along with the displacement in Figure S 20. In order to maintain the original shape of the nanostructure the whole nanostructure has been fixed. In order to compare the separation behavior of spiral structures with a flat structure such as CNT, the separation behavior of (8,0) CNT with diameter of 6.2 A approximately equal to that of (2,1,2,1) SCBN has been investigated. It is concluded that the sliding mode separation of CNT involves three stages. In the first stage, the force per atom increases dramatically to about 10 Angstroms. Following the process of separation and into stage two, the force oscillates approximately around the maximum force. In the third stage, the force per atom decrease dramatically and reaches zero value. The mentioned stages show a good agreement with the previous researches[2-4, 18-20]. Also, the maximum force, separation energy and final displacement are presented in Table S 2. Moreover, separation energy per initial length and ISS are listed in Table S 2 in order to compare with other reported results and previous results[4, 18-20], respectively. The ISS (ζ) can be written:

$$\text{V}E_{po} = \int_0^L F(x)dx \qquad (1)$$

$$F(x) = 2\pi r(L-x)\zeta \qquad (2)$$

$$\zeta = \text{V}E_{po} / \pi r L^2 \qquad (3)$$

where L is the initial length of CNT, and r is radius of CNT. The calculated ISS (100.7 MPa) is in agreement with previous researches[4, 18-20] which are calculated ISS with different methods. In addition, the separation energy per initial length of CNT is much smaller than that of (2,1,2,1) SCBN which has equal diameter to the CNT.

Table S 3. Force per atom, separation energy, ISS and final displacement for (8,0) CNT.

Structural type	ISS (MPa)	Max-Force per atom (pN)	Separation Energy (mJ/m^2)	Max-Traction (GPa)	Final displacement (A)	Separation Energy per initial length (mJ/m^3)
(8,0) CNT	100.71	1.7769	186.3155	0.07	52.4	5.035

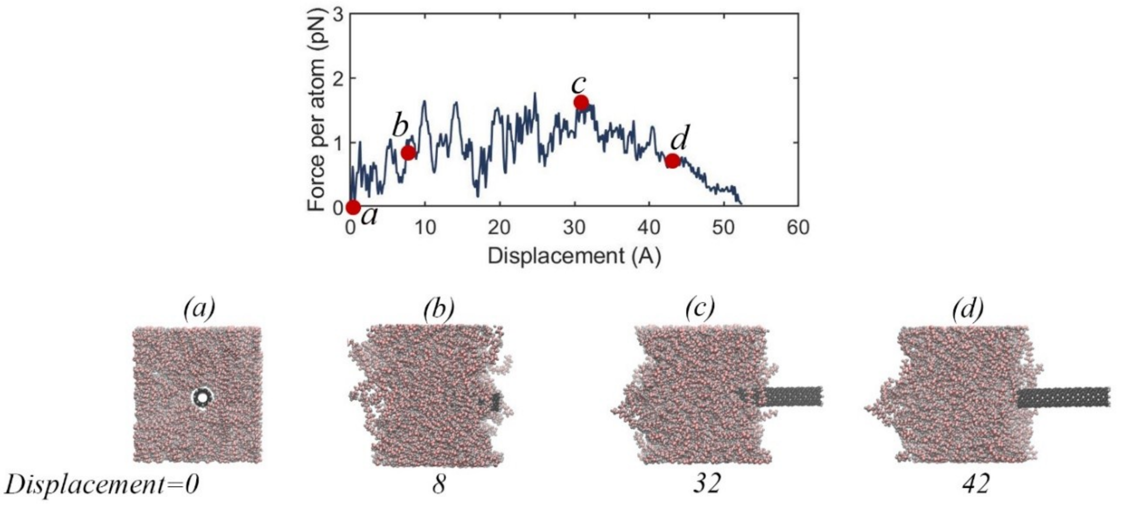

Figure S 20. The force per atom-displacement diagram for sliding mode separation of CNT. The interaction of CNT and polyethylene is shown in different displacements.

S20. The unconstrained/constrained area of simulation box during pullout test.

Figure S 21 shows the unconstrained/constrained area of simulation box during the pullout test. To illustrate the details, only the unconstrained/constrained area is shown in one direction.

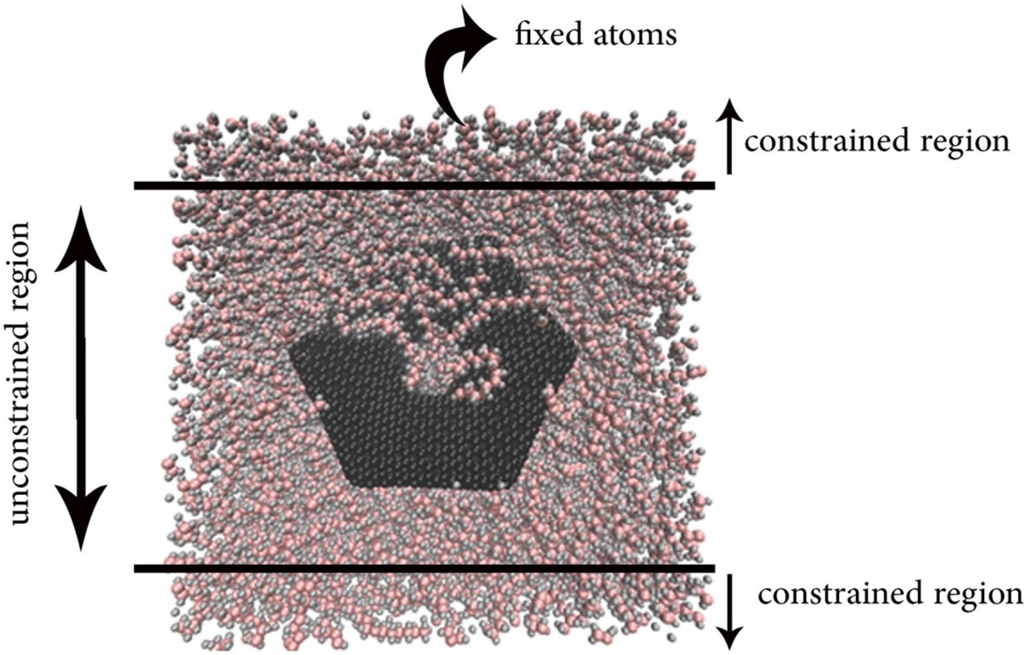

Figure S 21. The unconstrained/constrained area of simulation box during pullout test.

References

[1] Li Y,Seidel G. *Multiscale modeling of functionalized interface effects on the effective elastic material properties of CNT–polyethylene nanocomposites.* Computational Materials Science 2015; 107:216-34.

[2] Li Y,Seidel G D. *Multiscale modeling of the effects of nanoscale load transfer on the effective elastic properties of unfunctionalized carbon nanotube–polyethylene nanocomposites.* Modelling and Simulation in Materials Science and Engineering 2014; 22(2):025023.

[3] Awasthi A P, Lagoudas D C,Hammerand D C. *Modeling of graphene–polymer interfacial mechanical behavior using molecular dynamics.* Modelling and Simulation in Materials Science and Engineering 2008; 17(1):015002.

[4] Zhan H, Zhang G, Tan V B, Cheng Y, Bell J M, Zhang Y W, et al. *Diamond nanothread as a new reinforcement for nanocomposites.* Advanced Functional Materials 2016; 26(29):5279-83.

[5] Meirovitch H. *Computer simulation of self-avoiding walks: Testing the scanning method.* The Journal of Chemical Physics 1983; 79(1):502-8.

[6] Dechant J. *Polymer handbook. J. BRANDRUP and EH IMMERGUT (editors). ISBN 0-471-81244-7. New York/Chichester/Brisbane/Toronto/Singapore: John Wiley & Sons 1989. Cloth bond, ca. 1850 pages,£ 115.00, $175.00.* Acta Polymerica 1990; 41(6):361-2.

[7] Li M, Zhou H, Zhang Y, Liao Y,Zhou H. *The effect of defects on the interfacial mechanical properties of graphene/epoxy composites.* RSC Advances 2017; 7(73):46101-8.

[8] Stuart S J, Tutein A B,Harrison J A. *A reactive potential for hydrocarbons with intermolecular interactions.* The Journal of Chemical Physics 2000; 112(14):6472-86.

[9] Wang J, Kemper T, Liang T,Sinnott S B. *Predicted mechanical properties of a coiled carbon nanotube.* Carbon 2012; 50(3):968-76.

[10] Sinnott S B, Colton R J, White C T,Brenner D W. *Surface patterning by atomically-controlled chemical forces: molecular dynamics simulations.* Surface Science 1994; 316(1-2):L1055-L60.

[11] Wijesundara M B, Hanley L, Ni B,Sinnott S B. *Effects of unique ion chemistry on thin-film growth by plasma–surface interactions.* Proceedings of the National Academy of Sciences 2000; 97(1):23-7.

[12] Qi L,Sinnott S B. *Polymerization via Cluster− Solid Surface Impacts: Molecular Dynamics Simulations.* The Journal of Physical Chemistry B 1997; 101(35):6883-90.

[13] Safaei M, Sheidaei A, Baniassadi M, Ahzi S, Mashhadi M M,Pourboghrat F. *An interfacial debonding-induced damage model for graphite nanoplatelet polymer composites.* Computational Materials Science 2015; 96:191-9.

[14] Yousefi E, Sheidaei A, Mahdavi M, Baniassadi M, Baghani M,Faraji G. *Effect of nanofiller geometry on the energy absorption capability of coiled carbon nanotube composite material.* Composites Science and Technology 2017; 153:222-31.

[15] Sharifian A, Baghani M, Wu J, Odegard G M,Baniassadi M. *Insight into Geometry-Controlled Mechanical Properties of Spiral Carbon-Based Nanostructures.* The Journal of Physical Chemistry C 2019; 123(5):3226-38.

[16] Sharifian A, Moshfegh A, Javadzadegan A, Afrouzi H H, Baghani M,Baniassadi M. *Hydrogenation-Controlled Mechanical Properties in Graphene Helicoids: Exceptionally Distribution-Dependent Behavior.* Physical Chemistry Chemical Physics 2019; 21(23):12423-33.

[17] Wu J, Zhao H, Liu J, Zhang Z, Ning F,Liu Y. *Nanotube-chirality-controlled tensile characteristics in coiled carbon metastructures.* Carbon 2018; 133:335-49.

[18] Zheng Q, Xia D, Xue Q, Yan K, Gao X,Li Q. *Computational analysis of effect of modification on the interfacial characteristics of a carbon nanotube–polyethylene composite system.* Applied Surface Science 2009; 255(6):3534-43.

[19] Li Y, Liu Y, Peng X, Yan C, Liu S,Hu N. *Pull-out simulations on interfacial properties of carbon nanotube-reinforced polymer nanocomposites.* Computational Materials Science 2011; 50(6):1854-60.

[20] Haghighatpanah S,Bolton K. *Molecular-level computational studies of single wall carbon nanotube–polyethylene composites.* Computational Materials Science 2013; 69:443-54.